Fluxon pinning through interaction with the superconducting wiring of long annular Josephson junctions

D. Münter, T. Doderer,* H. Preßler,† S. Keil, and R. P. Huebener

Physikalisches Institut, Lehrstuhl Experimentalphysik II, Universität Tübingen, Auf der Morgenstelle 14, D-72076 Tübingen, Germany

(Received 11 May 1998)

The statics and dynamics of magnetic-flux quanta (fluxons) in long annular Josephson tunnel junctions have been investigated. Pinning by interaction of the fluxon field outside the junction with the superconducting wiring has been observed in spatially resolving measurements using low-temperature scanning electron microscopy. We were able to influence the characteristics of this field by carefully modifying the beam-induced fluxon trapping procedure. In this way we were able to select the pinning site acting on the fluxon. [S0163-1829(98)04145-9]

I. INTRODUCTION

The nonlinear system constituted by a Josephson tunnel junction has served as a rich source of interesting physical phenomena over the past decades.[1] Especially long junctions, i.e., junctions with at least one dimension large against the Josephson penetration depth λ_j, have proven to be a suitable tool for the investigation of soliton (fluxon) statics and dynamics. Most of the experimental work was carried out on linear Josephson junctions in the inline or overlap geometry.[2] The samples used for the experiments described in this article were of annular quasi-one-dimensional shape and are characterized in detail in Sec. II.

One-dimensional long Josephson junctions are governed by the perturbed sine-Gordon equation[3]

$$\varphi_{xx} - \varphi_{tt} = \sin\varphi + \alpha\varphi_t - \beta\varphi_{xxt} - \gamma + f(x,\varphi), \qquad (1)$$

where $\varphi(x,t)$ is the spatially and time-dependent phase difference across the tunnel barrier between the two Cooper pair systems of the superconducting electrodes. In the case of annular Josephson junctions, x runs azimuthally around the junction. The variables x and t are normalized to the Josephson penetration depth λ_j and the inverse of the plasma frequency ω_p^{-1}, respectively. The dissipation parameters α and β account for losses due to quasiparticle currents across and parallel to the tunnel barrier, respectively, whereas γ represents the normalized bias current. The function $f(x,\varphi)$ describes inhomogeneities of various origins, such as externally applied magnetic fields or local changes of the thickness of the insulating barrier (e.g., microshorts). For annular junctions the dynamics and statics of solitons in the presence of inhomogeneities have already been investigated experimentally and numerically.[3–7] Because strictly speaking the term "soliton" only refers to certain exact solutions of the *unperturbed* sine-Gordon equation, we use the word "fluxon" from this point on. In the annular geometry the boundary conditions for Eq. (1) are periodic, i.e.,

$$\varphi(l,t) = \varphi(0,t) + n2\pi, \quad \varphi_x(l,t) = \varphi_x(0,t), \qquad (2)$$

where l is the ring circumference in units of λ_j and n is the net number of fluxons trapped in the junction. This means that there can only be an integer number of fluxons inside the junction at any given time. If each of the two superconducting junction electrodes is thicker than the magnetic penetration depth λ_L (which is the case for the samples studied here), the total magnetic flux and thus the net fluxon number in the annular junction is conserved. This conservation and the fact, that fluxons can move inside the junctions without influence of boundaries have motivated the experiments with annular junctions.

Even though there have been investigations to determine the behavior of fluxons in externally applied magnetic fields, there have been no experiments so far, to our knowledge, considering the fluxon magnetic field outside the actual junction. In our experiments we found evidence that an interaction of this field with the superconducting wiring takes place and results in a pinning potential when junctions of the "Lyngby geometry"[8] are used, as is the case in most of the studies in the literature. We have also investigated the single-fluxon statics in this potential by means of low-temperature scanning electron microscopy (LTSEM) which allows a spatially resolved measurement of the Josephson current. These results are presented in Sec. III. Moreover, we discovered consequences of this pinning in the dynamics of multifluxon systems to the degree that a consecutive transition of the fluxons into the dynamic state was observed as described in Sec. IV.

II. THE SAMPLES AND THE EXPERIMENTAL SETUP

The samples that have been used for our measurements are Nb/AlO$_x$/Nb tunnel junctions[9] with the annular geometry introduced by the Lyngby group (see Fig. 1).[8] The current density j_c at 4.2 K of these junctions is 1000 A/cm^2, the mean radius is 90 μm. The width of the rings is 10 μm (sample A) and 5 μm (sample B), respectively. The circumference of the ring, being the junction length, is 565 μm for both samples, corresponding to about 49 λ_j. This is very long compared to most other experiments conducted with annular junctions. This fact turns out to be vital for the observation of the phenomena described in this article. At 4.2 K the critical currents of the samples are approximately 45 mA (sample A) and 23 mA (sample B). The zero field step asymptotic voltages were measured to be about 30 μV at 4.2 K.
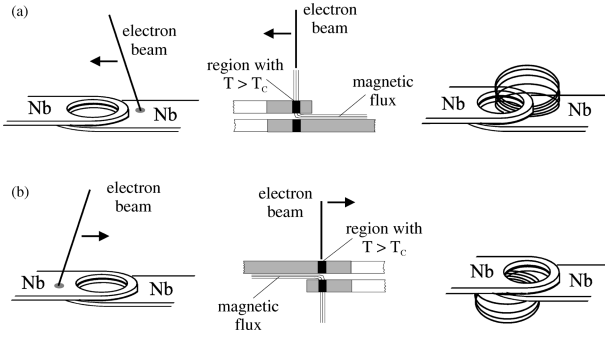
FIG. 1. Schematic representation of the trapping procedures for fluxons resulting in a defined extrajunctional magnetic field configuration. The electron beam is switched on when already focused on one of the electrodes. The energy deposited by the electron beam results in local heating to temperatures above T_c. Magnetic flux can only penetrate the normal region in the electrode crossed second by the beam. (a) shows the procedure starting from the bottom electrode, (b) from the top electrode.

We performed spatially resolved measurements by means of low-temperature scanning electron microscopy.[10,11] LTSEM allows the local thermal perturbation of the junction due to the electron beam with the focus at x_0 during operation of the sample at liquid helium temperatures. The spatial extension of this perturbation is given by the thermal healing length and its value determines the spatial resolution, being about $1-2$ μm for the samples studied here. The beam-induced temperature increment $\Delta T(x_0)$ can be tuned by the electron beam power. Since the thermal relaxation time for the beam induced local thermal perturbation is about 100 ns, the sample response signal is a time averaged information about the junction dynamics. The latter evolve on a time scale of about 10 ps.

In this article we present two different imaging techniques for the pinned fluxons. The first method uses the electron beam induced additional energy loss during the collision of two fluxons. In the case of fluxon-antifluxon collisions a significant electron beam induced voltage signal $\Delta V(x_0) < 0$ of the current-biased junction at the collision sites can be observed.[12,13] Notice, that we are dealing with the collision of fluxons of the same polarity in contrast to the fluxon-antifluxon collisions considered in Refs. 12 and 13. Our experimental results show that also in the case of the collision of unipolar fluxons, the local thermal perturbation due to the electron beam causes a significant sample response $\Delta V(x_0) < 0$ at the collision sites, as has been already observed by Keil $et\ al.$[4]

The second method is based on the two-dimensional imaging of the spatial distribution of the maximum dc Josephson current density[14,15]

$$j(x) = j_c(x) \sin \varphi(x) \qquad (3)$$

depending on j_c and on the phase difference φ. In our case, where j_c does not show any significant spatial dependence across the junction,[16] $j(x)$ is directly proportional to $\sin \varphi(x)$. The local thermal perturbation induced by the electron beam at x_0 decreases $j_c(x_0)$ and, neglecting any nonlocal effect, the change $\Delta j(x_0)$ is a direct measure of $\sin\varphi(x_0)$.[14] The junction is biased close to the total critical current

$$I_c \approx I = \int_0^l j_c \sin \varphi(x)\, dx \qquad (4)$$

and I_c is continuously measured during scanning the e beam across the sample. We obtain the electron-beam-induced signal

$$-\Delta I_c(x_0) \propto \sin \varphi(x_0), \qquad (5)$$

if the area perturbed by the beam is small compared to λ_j. In case of a hysteretic current-voltage characteristic (IVC) this imaging technique is described in Ref. 14, whereas for a nonhysteretic IVC a description of the imaging technique can be found in Ref. 15. For all images shown in this article any nonlocal effect of the local perturbation due to the macroscopic quantum properties of a Josephson junction can be ruled out.[17] For a comprehensive review of the imaging of Josephson junction dynamics see Ref. 18.

III. SINGLE-FLUXON EXPERIMENTS

The key prerequisite for studying fluxon motion in annular Josephson junctions is fluxon trapping. For this purpose one has to break superconductivity. In addition, a magnetic field has to be applied during cooling of the sample through T_c. One or more fluxons can be trapped during this procedure. There are several methods for fluxon trapping.[19,20] Since in a scanning electron microscope we investigate the cold samples, a reliable way of introducing fluxons into the junction consists of locally heating the superconducting electrodes to a temperature above T_c by electron beam irradiation. A magnetic field can be applied during cooling by passing some current through the junction or by means of an external solenoid. In our experiments we found it favorable to apply an external field to achieve controllable trapping of single fluxons. Figure 1 shows schematically the procedure of introducing a fluxon into the junction. After the scanning unit of the LTSEM was adjusted to deflect the electrons onto one of the electrodes the beam was switched on. This operation guarantees that the area heated above T_c by the beam does not contain any magnetic flux because it is generated well apart from the edges in the superconducting material. Subsequently, when the electron beam is moved towards the center of the ring, the second electrode is heated as well. In this electrode magnetic flux supplied by the external field can be dragged along. Note that the different starting points depicted in Figs. 1(a) and 1(b) lead to different configurations of the external fluxon field. Inside the junction the results of the two procedures are identical.

After fluxon trapping, the number of trapped fluxons can easily be determined experimentally by recording the IVC of the junction through applying a current to the junction. Due to the Lorentz force between the bias current and the magnetic moment of the fluxon the latter is accelerated, moves through the junction, and a voltage drop is observed. The IVC of sample A with one fluxon trapped by the procedure described above is shown in Fig. 2(a) as well as the differential resistance (dU/dI) measured through electronic differentiation with a lock-in amplifier. The asymptotic voltage of about 30 μV corresponds to the limiting Swihart velocity $\bar{c}$,[21] the velocity of light in the junction transmission line. Note that the curvature of the IVC does not comply with

MÜNTER, DODERER, PREßLER, KEIL, AND HUEBENER
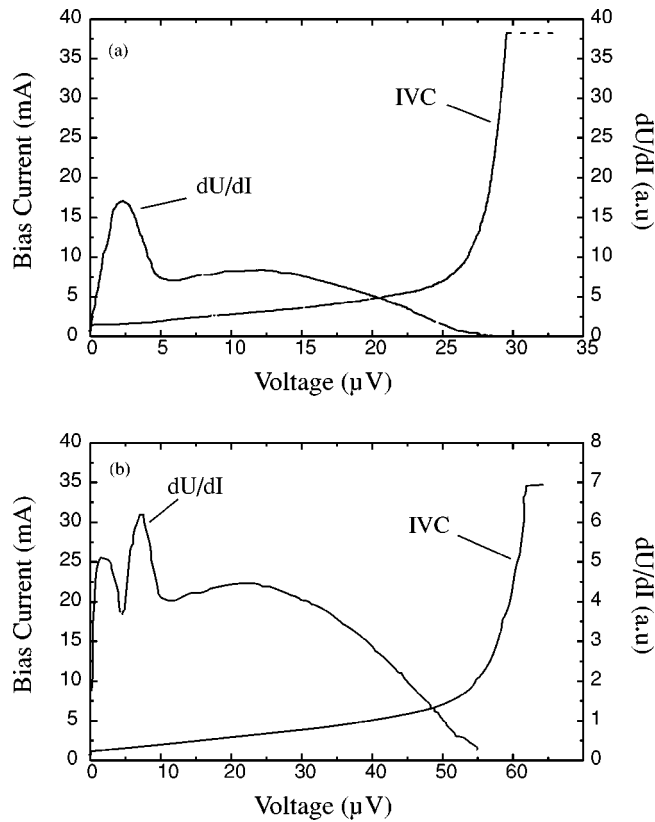
FIG. 2. Current-voltage curve (IVC) and differential resistance (dU/dI) of the annular junction (sample A) with (a) one fluxon and (b) two fluxons trapped using the trapping procedure of Fig. 1(a). Small critical currents of about 1 mA and 0.6 mA, respectively (approx. 3% of I_c with no fluxon) and the peaks in the dU/dI curves are evidence of fluxon pinning. $T \approx 4.2$ K.

perturbation theory, which predicts $d^2U/dI^2 < 1$ for all V. We believe that the reason for this is the voltage dependency of the quasiparticle tunneling probability,[22] which means that the dissipation parameter α is voltage dependent as well.

The small critical current of about 1 mA (roughly 3% of I_c without fluxons trapped) suggests the existence of a pinning potential. Various authors have reported similar observations.[8,23–25] Davidson *et al.* found a small critical current for the IVC of a junction with a length of 15 λ_j when fluxons were trapped. That critical current depended on the junction history.[8]

The statics of a single fluxon in the pinning potential responsible for the small critical current described above was investigated by LTSEM. In Figs. 3(b) and 3(c) LTSEM images of a single fluxon trapped by the procedure depicted in Fig. 1(a) are shown (sample A). They show a single fluxon at two different positions in the ring. The white areas correspond to a Josephson supercurrent into the paper plane, the black areas into the opposite direction. The magnetic moment and the direction in which the Lorentz force acts are symbolized by arrows. Apparently the location of the pinning center depends on the direction of the bias current. Considering that, because of the way the fluxon was trapped, the magnetic field of the fluxon encloses only the upper electrode [see Fig. 1 (a)]. Therefore, we conclude that the fluxon gets pinned through the interaction with the upper electrode.

Further evidence for the validity of this argument is given
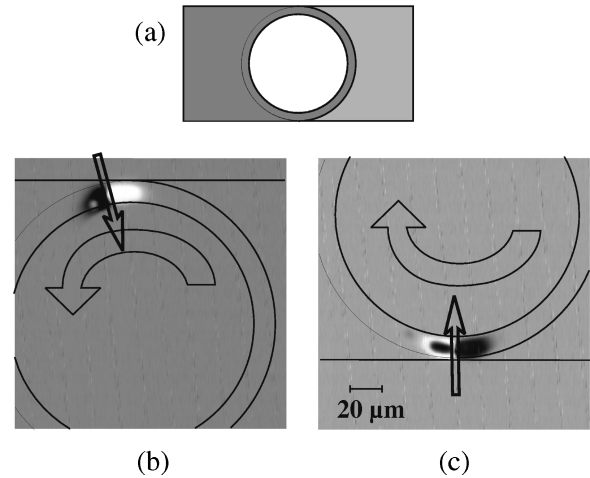
FIG. 3. (a) Sketch of the annular junction with the same orientation as in (b) and (c) but drawn to different scale. The voltage images in (b) and (c) show a single static fluxon trapped by the procedure of Fig 1(a) (sample A). For imaging, the junction was biased at $I = +1.9$ mA and $I = -2.2$ mA, respectively. Positive bias current values denote a current flow from the top to the bottom electrode. Fluxon magnetic moment and the direction of the Lorentz force are symbolized by arrows.

by the LTSEM images of Fig. 4. The fluxon shown in these images was trapped in the junction using the procedure depicted in Fig. 1(b) (sample A). Hence the magnetic field of the fluxon encloses only the lower electrode and gets caught on that wiring when acted on by the bias current. The fact, that the position of the pinned fluxons with respect to the horizontal symmetry axis of the junction differs for reverse bias current directions in both Figs. 3 and 4, hints at the existence of additional forces on the fluxon. The measurements took place in a reasonably well shielded environment. However it is possible, that some external magnetic field is present at the sample site, which would act as an additional pinning force.

An investigation of single fluxons trapped in the junction by crossing both electrodes *from the side*, i.e., switching on the electron beam outside the electrodes and then moving it into the center of the ring by crossing the narrowest part of the combined electrodes, confirms the above interpretation. This procedure allows the field of the fluxon to circle both electrodes as schematically shown in Fig. 5. Even though
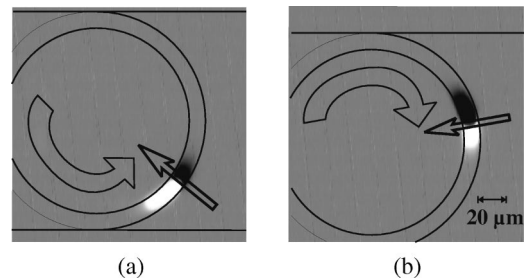
FIG. 4. LTSEM voltage images of a single static fluxon trapped by the procedure depicted in Fig. 1(b). The junction (sample A) was biased at $I = +1.7$ mA (a) and $I = -1.6$ mA (b), respectively. In contrast to the single-fluxon configuration shown in Fig. 3 pinning at the edges of the lower electrodes can be observed [sample orientation as shown in Fig. 3(a)].
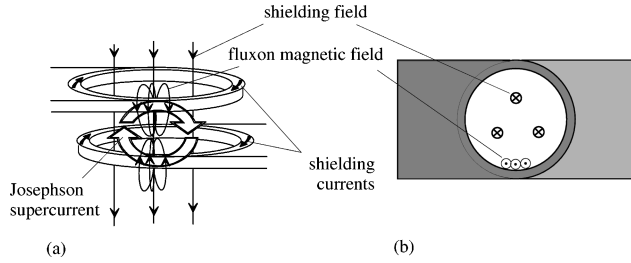
FIG. 5. (a) Schematic drawing of a possible extrajunctional field configuration for the case of a fluxon trapped by crossing both electrodes simultaneously with the focused electron beam at their narrowest point, i.e., along the vertical symmetry axis in Fig. 3(a). Shielding currents in the electrodes are necessary to ensure the unambiguity of the Cooper pair wave functions, which results in flux quantization in the rings of the electrodes. (b) Sketch of the flux distribution for the upper electrode in the situation depicted in (a). Even though the net flux in the opening $\Phi_{net}=0$, the fluxon magnetic field outside the junction will still interact with both wirings.

shielding currents flow in the electrodes to ensure the unambiguity of the Cooper pair function in each electrode (the magnetic flux contained by a single fluxon is exactly the elementary flux quantum Φ_0), pinning is still expected to occur. The reason is the fluxon field outside the junction in the shape of a distorted magnetic dipole field having its maximum value just at the outer border of the junction [see Fig. 5(b)]. The distortion is due to the Meissner effect in the superconducting electrodes. Inside the junction the fluxon field is localized to an azimuthal length comparable to the Josephson penetration depth. In this case interaction of the fluxon magnetic field with the wiring of both electrodes takes place. The resulting pinning potential is expected to be shallower than the potential discussed earlier for the procedures in Figs. 1(a) and 1(b). Consequently the critical current should be lower. Experiments showed indeed, that trapping of single fluxons over the sides resulted in a value of I_c being 50% smaller than for trapping from the middle of the electrodes.

It is interesting that the transition into the dynamic state does not happen in an abrupt manner. Even if a significant voltage drop is measured across the junction for a single-fluxon mode [for example, a voltage greater than 5 μV in Fig. 2(a)] the LTSEM images (not shown here) still display the Josephson current distribution of a fluxon at rest. We believe that this is a result of the relatively weak pinning forces which allow the fluxon to get depinned only part of the time at first. As described in Sec. II the LTSEM images are time averaged measurements. Therefore, the images recorded at finite voltages can be interpreted as time averaged images of a sporadically moving fluxon.

IV. MULTIFLUXON EXPERIMENTS

The features of IVC's do not change qualitatively when more than one fluxon is trapped. Figure 2(b) shows the IVC and the differential resistance for the case of two fluxons trapped by the procedure shown in Fig 1(a). The dU/dI-curve displays two peaks at low voltages corresponding to the consecutive transition of the two fluxons from the static into the dynamic state. Note that I_c of the two fluxon
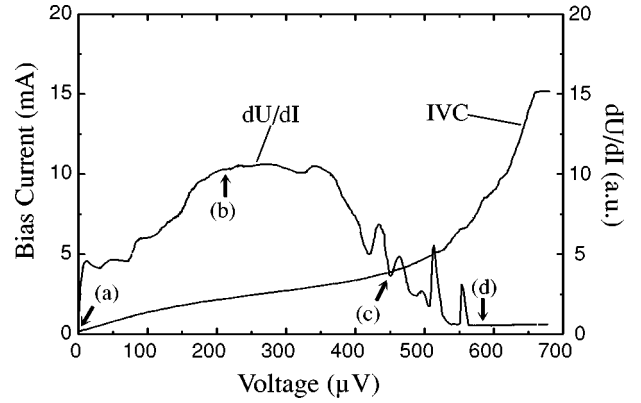
FIG. 6. Current-voltage characteristic (IVC) and differential resistance (dU/dI) of the junction (sample B) with 17 fluxons trapped. Due to a small ohmic resistance in series with the junction the IVC is tilted. The peaks in the dU/dI curve are a result of the consecutive transition of the fluxons from the static to the dynamic state. The arrows indicate the voltages at which the LTSEM images in Fig. 7 were recorded.

system is only about 60% of the value for one fluxon. It appears that this is due to the interfluxon repulsion of the fluxon magnetic moments.[4]

In light of the concentration of the extrajunctional fluxon field in the immediate vicinity of the junction [see Fig. 5 (b)] it is noteworthy that it was not possible to trap more than seven fluxons in the junction by repeatedly applying the procedures shown in Fig 1. On the other hand, only a little effort was needed to trap up to 50 fluxons by introducing them over the sides, i.e., allowing the fluxon magnetic field to enclose both electrodes.[25] As already explained in Sec. III (reduced) pinning is still expected for this case. The IVC and the dU/dI curve for such a multifluxon mode show a rather complicated shape as depicted in Fig. 6 for the situation of 17 fluxons trapped in the junction (sample B). Due to the presence of a small ohmic resistance in series with the junction in this particular measurement the IVC is tilted and the asymptotic voltage is larger than the 510 μV expected for a 17 fluxon system. Nevertheless the structure of the dU/dI curve can be explained by the consecutive transition of all 17 fluxons from the static into the dynamic state.

Fluxon-fluxon collisions are expected for the situation where more than one fluxon is trapped in the junction, while at least one of them is moving and the others are pinned. A large number of LTSEM images were recorded near the resonant structures in Fig. 6. Arrows indicate the voltages at which selected images, shown in Fig. 7, were taken. In the LTSEM images we observe the following process. One after another the fluxons get depinned when the bias current is increased, as indicated by the decreasing number of signal peaks. Finally only a single one is still at rest while 16 are moving as seen in Fig. 7(d). The moving fluxons are used as a detector for the pinned ones by the collisions that take place once during each revolution of every moving fluxon.

At this point it is necessary to recall that the transition into the dynamic state is not abrupt. Instead a sporadic change between statics and dynamics of a particular fluxon takes place. Therefore it makes sense that the image in Fig. 7(d) still shows the last fluxon, even though it was recorded at a voltage greater than the one corresponding to the last
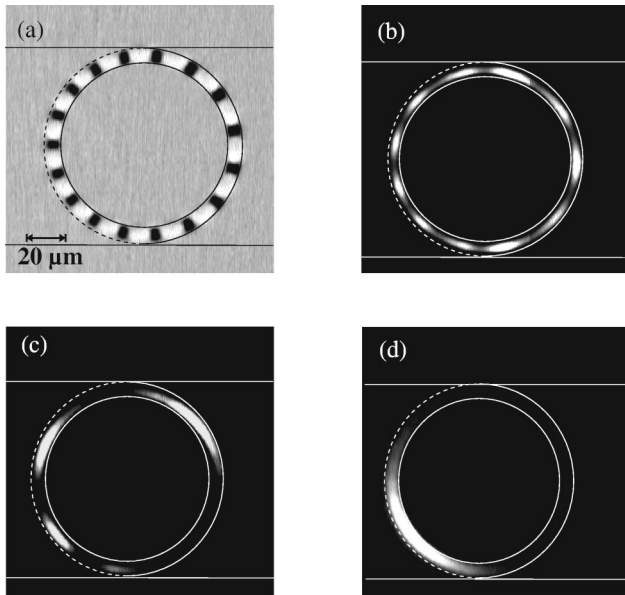
FIG. 7. LTSEM voltage images of 17 fluxons trapped in the junction (sample B) at different bias current values. [Sample orientation as shown in Fig. 3(a).] (a) All 17 fluxons are at rest. The size of the fluxons is reduced compared to the single-fluxon case of Figs. 3 and 4 due to fluxon compression inside the junction. (b) At $I = 2.1$ mA the image still shows eleven signal peaks, indicating that six fluxons are moving. (c) Four peaks are left at a bias current $I = 3.6$ mA. (d) Finally at $I = 7.3$ mA only a single static fluxon is visible.

peak in the differential resistance in Fig. 6. This is in accordance with the findings for single trapped fluxons. It is interesting that the position of the last static fluxon shown in Fig. 7(d) is identical with the one of a single fluxon getting pinned at the wiring of the upper electrode. For reversed bias

current direction the pinning of the last fluxon at the other side of the same wiring was observed.

Furthermore we want to point out the way in which the size of the fluxons is different in each of the images of Fig. 7. The fluxon compression [see Eq. (2)] results in a reduced fluxon length, since the fluxons are ''squeezed'' into the junction. The more fluxons change to the dynamic state, the less compression the static ones experience. Therefore the static fluxons expand. Finally the last static fluxon [Fig. 7 (d)] reaches the ''relaxed'' size, i.e., the size we observe if only a single fluxon exists in the junction at rest, being approximately $2\pi\lambda_j$.

V. CONCLUSIONS

We have investigated the statics and dynamics of (Josephson) fluxons in long annular $Nb/AlO_x/Nb$ tunnel junctions. The current-voltage characteristics showed evidence of fluxon pinning. Applying low-temperature scanning electron microscopy, we were able to image the statics of single pinned fluxons. By carefully controlling the procedure through which fluxons were introduced into the junction, it was possible to influence the position of the pinned fluxons. These experiments show that this pinning is a result of the interaction of the magnetic fluxon field with the superconducting wiring of the junction. We have also investigated the behavior of multifluxon states. For the case of 17 fluxons trapped in the junction we found that the fluxons get depinned one after another with increasing bias current.

*Present address: IBM T. J. Watson Research Center, Yorktown Heights, New York 10598.

†Present address: Electrotechnical Laboratory, Umezono 1-1-4, Tsukuba, 305, Japan.

[1] A. Barone and G. Paternó, *Physics and Applications of the Josephson Effect* (Wiley, New York, 1982).

[2] R. D. Parmentier, in *The New Superconducting Electronics*, edited by H. Weinstock and R. W. Ralston (Kluwer, Dordrecht, 1993), p. 221; N. F. Pedersen and A. V. Ustinov, Supercond. Sci. Technol. **8**, 389 (1995).

[3] D. W. McLaughlin and A. C. Scott, Phys. Rev. B **18**, 1652 (1978).

[4] S. Keil, I. V. Vernik, T. Doderer, A. Laub, H. Preßler, R. P. Huebener, N. Thyssen, A. V. Ustinov, and H. Kohlstedt, Phys. Rev. B **54**, 14 948 (1996).

[5] S. Keil, diploma thesis, University of Tübingen, 1996.

[6] N. Grønbech-Jensen, P. S. Lomdahl, and M. R. Samuelsen, Phys. Rev. B **43**, 12799 (1991).

[7] N. Martucciello and R. Monaco, Phys. Rev. B **53**, 3471 (1996).

[8] A. Davidson, B. Dueholm, B. Kryger, and N. F. Pedersen, Phys. Rev. Lett. **55**, 2059 (1985).

[9] The samples designed by the authors have been fabricated by

HYPRES Inc., Elmsford, NY 10523.

[10] R. P. Huebener, in *Advances in Electronics and Electron Physics*, edited by P. W. Hawkes (Academic, New York, 1988), Vol. 70, p. 1.

[11] R. Gross and D. Koelle, Rep. Prog. Phys. **57**, 651 (1994).

[12] A. Laub, T. Doderer, S. G. Lachenmann, R. P. Huebener, and V. A. Oboznov, Phys. Rev. Lett. **75**, 1372 (1995).

[13] S. G. Lachenmann, T. Doderer, R. P. Huebener, D. Quenter, J. Niemeyer, and R. Pöpel, Phys. Rev. B **48**, 3295 (1993).

[14] J. Bosch, R. Gross, M. Koyanagi, and R. P. Huebener, Phys. Rev. Lett. **54**, 1448 (1985); J. Low Temp. Phys. **68**, 245 (1987).

[15] D. Quenter, A. V. Ustinov, S. G. Lachenmann, T. Doderer, R. P. Huebener, F. Müller, J. Niemeyer, R. Pöpel, and T. Weimann, Phys. Rev. B **51**, 6542 (1995).

[16] This can be checked using LTSEM by measuring the spatial distribution of the quasiparticle tunneling current density across the junction.

[17] J.-J. Chang, C. H. Ho, and D. J. Scalapino, Phys. Rev. B **31**, 5826 (1985).

[18] T. Doderer, Int. J. Mod. Phys. B **11**, 1979 (1997).

[19] A. V. Ustinov, T. Doderer, B. Mayer, R. P. Huebener, and V. A. Oboznov, Europhys. Lett. **19**, 63 (1992).

[20] I. V. Vernik, N. Lazarides, M. P. Sǿrensen, A. V. Ustinov, N. F. Pedersen, and V. A. Oboznov, J. Appl. Phys. **79**, 7854 (1996).

[21] J. C. Swihart, J. Appl. Phys. **32**, 461 (1961).

[22] M. Tinkham, *Introduction to Superconductivity*, 2nd ed. (McGraw-Hill, New York, 1996).

[23] A. V. Ustinov, T. Doderer, R. P. Huebener, N. F. Pedersen, B. Mayer, and V. A. Oboznov, Phys. Rev. Lett. **69**, 1815 (1992).

[24] N. Martucciello, J. Mygind, V. P. Koshelets, A. V. Shchukin, L. V. Filippenko, and R. Monaco, Phys. Rev. B **57**, 5444 (1998).

[25] H. Preßler, diploma thesis, University of Tübingen, 1997.